



# A QUADRATIC LAYER ELEMENT FOR ANALYZING STRESS WAVES IN FGMS AND ITS APPLICATION IN MATERIAL CHARACTERIZATION

X. HAN, G. R. LIU AND K. Y. LAM

*Centre for Advanced Computations in Engineering Science (ACES), Department of Mechanical and Production Engineering, National University of Singapore, 10 Kent Ridge Crescent, Singapore 119260.  
E-mail: mpeliugr@nus.edu.sg*

AND

T. OHYOSHI

*Department of Mechanical Engineering, Akita University, Tegata, Akita City, Japan*

*(Received 12 June 1999, and in final form 1 February 2000)*

A novel method is presented for investigating elastic waves in functionally graded material (FGM) plates excited by plane pressure waves. The FGM plate is first divided into quadratic layer elements (QLEs). A general solution for the equation of motion governing the QLE has been derived. The general solution is then used together with the boundary and continuity conditions to obtain the displacement and stress in the frequency domain for an arbitrary FGM plate. The response of the plate to an incident pressure wave is obtained using the Fourier transform techniques. Results obtained by the present method are compared with an existing method using homogeneous layer elements. Numerical examples are presented to investigate stress waves in FGM plates. The relationship between the surface displacement response and the material property of quadratic FGM plates has been analytically obtained for the material characterization. A computational inverse technique is also presented for characterizing material property of an arbitrary FGM plate from the surface displacement response data, using present QLE method as forward solver and genetic algorithm as the inverse operator. This technique is utilized to reconstruct the material property of an actual SiC-C FGM.

© 2000 Academic Press

## 1. INTRODUCTION

Aircraft and spacecraft are typical weight-sensitive structures in which materials with high strength-to-weight and stiffness-to-weight ratios are required. Various advanced materials, such as composite materials have been developed and used in aircraft and spacecraft structures [1, 2]. Functionally graded materials (FGMs) have been proposed for thermal-protection systems of a space-plane. Many techniques [3, 4] have been developed for fabricating various FGMs, in which the material property changes continuously in the thickness direction. The FGM can be used not only in the thermal-protection systems of space-planes but also in electrical, chemical as well as many other fields.

Using elastic waves is one of the very promising means for material characterization of FGM. Effective use of elastic waves for such a purpose relies on a good understanding of wave propagation in FGMs. However, wave propagation problems related to FGM are

generally difficult to analyze without resorting to some numerical approaches, as the material property is function of the co-ordinates. There are a number of methods [5–9] for analyzing stress waves propagating in FGM plates. A brief review has been given by Liu *et al.* [10] on the existing methods for analyzing elastic-dynamic response of the FGM plate. Numerical models of FGM plates have been developed to solve forward problems that relate the material property to elastic wave fields. Thus, if a set of reasonably accurate experimentally measured response data is available, material property of FGM plate may be characterized by solving an inverse problem properly formulated, using forward solver.

In an inverse process, there are two very important factors affecting the performance. One is the number of the parameters to be reconstructed. The efficiency and accuracy of the results may reduce significantly, if the number of parameters is too large. Another factor is the efficiency of the forward solver, as it is usually called thousands of times in the inverse process.

Recently, a method has been proposed [10] using linearly inhomogeneous elements (LIEs) for analyzing stress waves in FGM. In an LIE, both the elastic constant and mass density are assumed to vary linearly in the thickness direction. It has been found that the material property can be approximated with piecewise linear functions. The LIE method can be used to solve forward problems that relate the material property to elastic wave fields in FGM plates. If the gradient constants, which represent the change of the material property of each LIE, are available, the material property of the whole FGM plate can be approximated in a discrete fashion. The characterization of material property of FGM is actually equivalent to characterize the gradient constants. It should be mentioned here that if LIEs are used, a sufficiently large number of elements are needed to accurately represent the variation of the material property of an arbitrary FGM plate. This translates to a large number of gradient constants to be reconstructed in an inverse process. Therefore, a high order element, such as a quadratic element, is very important, because it leads to a significant reduction in element numbers.

On the other hand, the material property does not change sharply in the thickness direction for many FGMs. In these cases, the material property may be approximated as quadratic functions. If a quadratic element can be developed, the whole plate can be modeled using a single element, and an explicit form of relationship between the material property and response of the FGM plate can be obtained. There is no need for an inverse process to characterize the material property of these FGMs. For an arbitrary FGM plate, using quadratic elements can reduce significantly the numbers of elements for representing the material variation, and less number of gradient constants needs to be reconstructed.

This paper consists two important parts. The first part is to propose a quadratic layer element method, based on quadratic approximation of material property in the thickness direction, for analyzing stress waves in FGM plate. Another is to suggest some analytical and numerical methods for characterizing material property of FGM using the present quadratic layer element (QLE) method.

## 2. A QUADRATIC LAYER ELEMENT METHOD

### 2.1. QUADRATIC LAYER ELEMENT

Consider a wave motion generated in an initially undisturbed, half-space FGM plate subjected to a plane stress wave. The FGM plate is divided into  $N$  quadratic layer elements

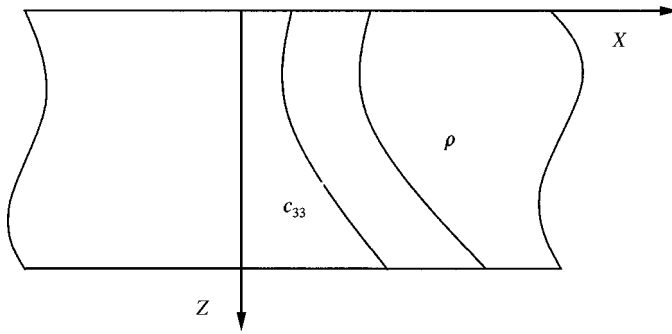


Figure 1. A quadratic layer element (QLE).

(QLEs) in the thickness direction. In each QLE,  $\rho$  and  $c_{33}$  are assumed to be quadratic functions of  $z$  shown in Figure 1:

$$\rho = \rho_0(1 + b_\rho z)^2, \quad c_{33} = c_{33}^0(1 + b_c z)^2, \tag{1}$$

where  $b_\rho$  and  $b_c$  are gradient constants representing the changing of material property within the QLE in the  $z$  direction.  $\rho_0$  and  $c_{33}^0$  are the mass density and the elastic constant of the material at the lower surface of the element.

Within a QLE, the governing differential equation (in the absence of body force) is given by

$$\frac{\partial}{\partial z} \left( c_{33} \frac{\partial w}{\partial z} \right) = \rho \frac{\partial^2 w}{\partial t^2}, \tag{2}$$

where  $\rho$  is the mass density and  $c_{33}$  is the elastic constant of the material. For isotropic materials, we have

$$c_{33} = \lambda + 2\mu, \tag{3}$$

where  $\lambda$  and  $\mu$  are lame constants. In equation (2),  $w$  is the displacement in the  $z$  direction.

It is assumed that the displacement in the frequency domain has the form

$$w = W(z) \exp(-i\omega t), \tag{4}$$

where  $\omega$  is the angular frequency. Substitution of equations (1) and (4) into equation (2), leads to the following equation:

$$(1 + b_c z)^2 \frac{d^2 W}{dz^2} + 2(b_c z + 1) b_c \frac{dW}{dz} + \frac{\rho_0 \omega^2}{c_{33}^0} (1 + b_\rho z)^2 W = 0. \tag{5}$$

Equation (5) can be rewritten as

$$\xi^2 \frac{d^2 W}{d\xi^2} + 2\xi \frac{dW}{d\xi} + (A_\xi \xi^2 + B_\xi \xi + C_\xi) W = 0 \tag{6}$$

in which the following substitutions have been made:

$$\xi = 1 + b_c z, \tag{7}$$

$$A_\xi = \frac{\omega^2 \rho_0 b_\rho^2}{c_{33}^0 b_c^4}, \quad (8)$$

$$B_\xi = \frac{2\omega^2 \rho_0 b_\rho}{b_c^3 c_{33}^0} - \frac{2\omega^2 \rho_0 b_\rho^2}{c_{33}^0 b_c^4}, \quad (9)$$

$$C_\xi = \frac{\omega^2 \rho_0}{c_{33}^0 b_c^2} - \frac{2\omega^2 \rho_0 b_\rho}{b_c^3 c_{33}^0} + \frac{\omega^2 \rho_0 b_\rho^2}{c_{33}^0 b_c^4}. \quad (10)$$

For FGMs,  $b_c \neq 0$ , but  $b_\rho$  may equal zero for some cases, such as layered structures [9, 11].

For  $b_\rho \neq 0$ , equation (6) can be rewritten as

$$\xi \frac{d^2 y}{d\xi^2} + 2(1+k) \frac{dy}{d\xi} + (A_\xi \xi + B_\xi) y = 0, \quad (11)$$

where

$$y = \xi^{-k} W \quad (12)$$

$$k = \frac{-1 \pm \sqrt{1 - 4C_\xi}}{2}. \quad (13)$$

Equation (11) has an exact solution in the form of confluent hypergeometric functions [12]:

$$W = \xi^k e^{D\xi/2} (A\phi(a, b, -D\xi) + B\varphi(a, b, -D\xi)), \quad (14)$$

where  $A$  and  $B$  are integral constants to be determined by the boundary conditions, and

$$D^2 = -4A_\xi, \quad h = D/2, \quad a = 1 + k + B_\xi/D, \quad b = 2 + 2k. \quad (15)$$

The functions  $\phi$  and  $\varphi$  in equation (14) are the confluent hypergeometric functions.

Using the displacement given in equation (14), the normal stress can be obtained

$$\sigma = AA^* + BB^*, \quad (16)$$

where

$$A^* = c_{33}^0 \xi^{k+1} e^{h\xi} \left( (\xi h + k) \phi(a, b, -D\xi) - \frac{2ah}{b} \xi \phi(a+1, b+1, -D\xi) \right) b_c, \quad (17)$$

$$B^* = c_{33}^0 \xi^{k+1} e^{h\xi} ((\xi h + k) \varphi(a, b, -D\xi) + 2ah\xi \varphi(a+1, b+1, -D\xi)) b_c. \quad (18)$$

For  $b_\rho = 0$ , equation (6) can be reduced to the following Euler equation:

$$\xi^2 \frac{d^2 W}{d\xi^2} + 2\xi \frac{dW}{d\xi} + C_\xi W = 0. \quad (19)$$

Equation (19) is a partial differential equation of second order with variable coefficients. The solution of equation (19) can be obtained in the form of [12]

$$W = \begin{cases} A\xi^{m_1} + B\xi^{m_2} & r' > 0, \\ A\xi^{-0.5} + B\xi^{-0.5} \ln|\xi| & r = 0, \\ \xi^{-0.5} (A \sin(\ln|\xi| m') + B \cos(\ln|\xi| m')) & r' < 0, \end{cases} \quad (20)$$

where  $A$  and  $B$  are integral constants to be determined by the boundary conditions,  $m_1$  and  $m_2$  are the roots of following equation:

$$m^2 + m + C_\xi = 0 \tag{21}$$

and

$$r' = (1 - 4C_\xi), \tag{22}$$

$$m' = 0.5\sqrt{|1 - 4C_\xi|}. \tag{23}$$

The normal stress can be obtained using the displacement given in equation (20)

$$\sigma = \begin{cases} c_{33}^0 b_c \xi^2 (m_1 A \xi^{m_1} + m_2 B \xi^{m_2}), & r' > 0, \\ c_{33}^0 b_c \xi^{1.5} (-0.5A + (1 - 0.5 \ln |\xi|) B), & r' = 0, \\ c_{33}^0 b_c \xi^{1.5} ((\cos(\ln |\xi| m') m' - 0.5 \sin(\ln |\xi| m')) A, & r' < 0. \\ - (0.5 \cos(\ln |\xi| m') + m' \sin(\ln |\xi| m')) B) \end{cases} \tag{24}$$

Solutions given by equations (14) and (16) or (20) and (24) are then applicable for all the  $N$  elements. Consequently, there are  $2N$  constants to be determined by the boundary conditions at the surfaces of the plate and the continuity conditions at the interfaces between the elements.

## 2.2. BOUNDARY AND CONTINUITY CONDITIONS

For generality, we first assume that the plate is loaded on the two surfaces as well as the  $(N - 1)$  interfaces by a harmonic load with an angular frequency  $\omega$ . Hence, the amplitude of the external force vector can be written as follows:

$$\mathbf{T}^T = \{T_1, T_2, T_3, \dots, T_N, T_{N+1}\}, \tag{25}$$

where  $T_j$  is the amplitude of the external force acting at the  $j$ th interface,  $j = 1$  is for the lower surface, and  $j = N + 1$  is for the upper surface of the plate. The boundary and continuity conditions for the FGM plate can be written as follows:

On the lower surface of the plate

$$-\sigma_1^L = T_1. \tag{26}$$

At the interfaces

$$\sigma_n^U - \sigma_{n+1}^L = T_{n+1}, \quad w_n^U = w_{n+1}^L \quad \text{for } 1 \leq n \leq (N - 1). \tag{27}$$

On the upper surface of the plate

$$\sigma_N^U = T_{N+1}. \tag{28}$$

The subscripts indicate the element numbers and the superscripts “ $U$ ” and “ $L$ ” stand, respectively, for the upper and lower surfaces of the layer elements.

Assembling all the QLEs using equations (26)–(28), we obtain the following equation for the whole plate:

$$\mathbf{T} = \mathbf{KA}, \tag{29}$$

where  $\mathbf{T}$  is the total external force, and  $\mathbf{A}$  is a vector of constants for all the layer elements:

$$\mathbf{A}^T = \{A_1, B_1, A_2, B_2, \dots, A_N, B_N\}. \tag{30}$$

Matrix  $\mathbf{K}$  in equation (29) is given by

$$\mathbf{K} = \begin{bmatrix} -K_{E11} & -K_{E12} & 0 & 0 & 0 & 0 & \cdot & 0 \\ T_{E11} & T_{E12} & -P_{E11} & -P_{E12} & 0 & 0 & \cdot & 0 \\ e_{11} & e_{12} & -K_{E21} & -K_{E22} & 0 & 0 & \cdot & 0 \\ 0 & 0 & T_{E21} & T_{E22} & -P_{E21} & -P_{E22} & \cdot & 0 \\ 0 & 0 & e_{21} & e_{22} & -K_{E31} & -K_{E32} & \cdot & 0 \\ \cdot & \cdot & \cdot & \cdot & \cdot & \cdot & \cdot & 0 \\ \cdot & \cdot & \cdot & \cdot & \cdot & \cdot & \cdot & 0 \\ \cdot & \cdot & \cdot & \cdot & \cdot & \cdot & \cdot & \cdot \\ 0 & 0 & 0 & 0 & 0 & 0 & e_{N1} & e_{N2} \end{bmatrix}, \tag{31}$$

where

$$K_{En1} = c_{33}^0(n)e^{h_n} \left( (h_n + k_n) \phi(a_n, b_n, -D_n) - \frac{2a_n h_n}{b_n} \phi(a_n + 1, b_n + 1, -D_n) \right) b_c, \tag{32}$$

$$K_{En2} = c_{33}^0(n)e^{h_n} \left( (h_n + k_n) \varphi(a_n, b_n, -D_n) + 2a_n h_n \varphi(a_n + 1, b_n + 1, -D_n) \right) b_c, \tag{33}$$

$$T_{En1} = e^{h_n \zeta_n} \phi(a_n, b_n, -2h_n \zeta_n) \zeta_n^{k_n}, \tag{34}$$

$$T_{En2} = e^{h_n \zeta_n} \varphi(a_n, b_n, -2h_n \zeta_n) \zeta_n^{k_n}, \tag{35}$$

$$P_{En1} = e^{h_n} \phi(a_n, b_n, -2h_n), \tag{36}$$

$$P_{En2} = e^{h_n} \varphi(a_n, b_n, -2h_n), \tag{37}$$

$$e_{n1} = c_{33}^0(n) \zeta_n^{k_n + 1} e^{h_n \zeta_n} \left( (\zeta_n h_n + k_n) \phi(a_n, b_n, -D_n \zeta_n) - \frac{2a_n h_n}{b_n} \zeta_n \phi(a_n + 1, b_n + 1, -D_n \zeta_n) \right) b_c, \tag{38}$$

$$e_{n2} = c_{33}^0(n) \zeta_n^{k_n + 1} e^{h_n \zeta_n} \left( (\zeta_n h_n + k_n) \varphi(a_n, b_n, -D_n \zeta_n) + 2a_n h_n \zeta_n \varphi(a_n + 1, b_n + 1, -D_n \zeta_n) \right) b_c. \tag{39}$$

Here

$$\zeta_n = 1 + b_{c(n)} H(n). \tag{40}$$

It should be noted that equations (32)–(39) are obtained for  $b_\rho \neq 0$ . Similar equations are obtained for  $b_\rho = 0$ :

$$K_{En1} = c_{33}^0(n) b_n m_{1(n)}, \quad K_{En2} = c_{33}^0(n) b_{c(n)} m_{2(n)}, \tag{41}$$

$$T_{En1} = \zeta_n^{m_{1(n)}}, \quad T_{En2} = \zeta_n^{m_{2(n)}}, \tag{42}$$

$$P_{En1} = 1, \quad P_{En2} = 1, \tag{43}$$

$$e_{n1} = c_{33}^0(n) b_{c(n)} \zeta_n^{1+m_{1(n)}} m_{1(n)}, \quad e_{n2} = c_{33}^0(n) b_{c(n)} \zeta_n^{1+m_{2(n)}} m_{2(n)}. \tag{44}$$

Equations (41)–(44) are for the case of  $r' > 0$ . The corresponding equations for  $r' < 0$  and  $r' = 0$  are given as follows:

For  $r' = 0$

$$K_{En1} = -0.5c_{33}^0(n)b_{c(n)}, \quad K_{En2} = c_{33}^0 b_{c(n)}, \tag{45}$$

$$T_{En1} = \zeta_n^{-0.5}, \quad T_{En2} = \zeta_n^{-0.5} \ln |\zeta_n|, \tag{46}$$

$$P_{En1} = 1, \quad P_{En2} = 0, \tag{47}$$

$$e_{n1} = -0.5c_{33}^0(n)b_{c(n)}\zeta_n^{0.5}, \quad e_{n2} = c_{33}^0(n)\zeta_n^{0.5}b_{c(n)}(1 - 0.5 \ln |\zeta_n|). \tag{48}$$

For  $r' < 0$

$$K_{En1} = c_{33}^0(n) b_{c(n)} m'_n, \quad K_{En2} = -0.5c_{33}^0(n) b_{c(n)}, \tag{49}$$

$$T_{En1} = \zeta_n^{-0.5} \sin(\ln |\zeta_n| m'_n), \quad T_{En2} = \zeta_n^{-0.5} \cos \ln |\zeta_n| m'_n, \tag{50}$$

$$P_{En1} = 0, \quad P_{En2} = 1, \tag{51}$$

$$e_{n1} = c_{33}^0(n) b_{c(n)} \zeta_n^{0.5} (-0.5 \sin(\ln |\zeta_n| m'_n) + m'_n \cos(\ln |\zeta_n| m'_n)),$$

$$e_{n2} = -c_{33}^0(n) b_{c(n)} \zeta_n^{0.5} (0.5 \cos(\ln |\zeta_n| m'_n) + m'_n \sin(\ln |\zeta_n| m'_n)). \tag{52}$$

Solving equation (29), the constant vector **A** can be obtained, and the displacement and stress in the frequency domain for each QLE can be obtained, respectively, using equations (14) and (16) or equations (20) and (24).

### 2.3. RESPONSE IN THE TIME DOMAIN

Once the displacement in the frequency domain is known, the displacement in the time domain can be obtained by the Fourier superposition

$$w_t(t) = \frac{1}{2\pi} \int_{-\infty}^{\infty} W(\omega) \bar{P}(\omega) \exp(i\omega t) d\omega, \tag{53}$$

where

$$\bar{P}(\omega) = \int_0^{t_f} P(t) \exp(-i\omega t) dt \tag{54}$$

is the Fourier transform of the incident pressure wave. In equation (54),  $P(t)$  is the incident pressure wave upon the FGM plates. The time duration of the load is  $(0, t_f)$ . The integrals in equation (53) can be evaluated by ordinary routines using equally spaced sampling points together with the exponential window method [13–15]. To minimize the sampling points and achieve a good accuracy in the integration, an adaptive quadrature scheme suggested by Liu *et al.* [15] is employed to evaluate the integrals in equation (53). The stress in the time domain can be obtained in the same way as the displacement.

## 3. NUMERICAL EXAMPLES

A program is developed in FORTRAN to compute the wave field in a FGM plate excited by an incident wave pressure on the surface of the plate. In the computation, the following dimensionless parameters are used:

$$\begin{aligned} \bar{w} &= w/H, \quad \bar{z} = z/H, \quad \bar{p} = p/c_{33r}, \quad \bar{\sigma} = \sigma/c_{33r}, \quad \bar{c}_{33} = c_{33}/c_{33r}, \\ \bar{\omega} &= \omega H/c_r, \quad \bar{t} = tc_r/H, \quad \bar{\rho} = \rho/\rho_r, \quad \bar{b}_c = b_c H, \quad \bar{b}_\rho = b_\rho H, \end{aligned} \quad (55)$$

where  $c_{33r}$  ( $c_{33r} = c_r^2 \rho_r$ ),  $c_r$ ,  $\rho_r$  are respectively, the reference elastic constant, wave velocity, and density, and  $\bar{t} = 1$  is the time for the wave of velocity  $c_r$  travelling once over the thickness  $H$  of the plate. For quadratic FGM plates investigated here, the wave velocity at the middle surface is used as the reference wave velocity  $c_r$ .

The external force  $\mathbf{T}$  used in equation (15) should be

$$\mathbf{T} = \{0, 0, 0, \dots, 0, 0, 0, P\}, \quad (56)$$

where

$$P = P_0 \sin(\omega_f t) \quad (57)$$

is the incident pressure wave upon the upper surface. In this paper, we set  $\bar{P}_0 = 2.0$ , and  $\bar{\omega}_f = 2\pi$  and  $\bar{t}_f = 2\pi/\bar{\omega}_f = 1.0$ , namely the wave is one cycle of a sine function.

For an arbitrary FGM plate, two models shown in Figure 2 can be used. The first model is using homogeneous elements, and the second model is using QLEs. In order to validate the present method, the displacement in the frequency domain of a quadratic FGM plate is computed. Material property of the quadratic FGM plate varies quadratically in the thickness direction as defined by equation (1). Only one QLE is used to obtain the exact results, and the results are shown in Figure 3 together with those obtained by a method proposed by Liu *et al.* [16], in which the plate is divided into homogeneous layers. It can be seen from Figure 3 that many homogeneous elements have to be used in order to obtain a result with a reasonable accuracy.

In order to investigate how a stress wave propagates in an FGM plate, the time history of the stress in a FGM plate subjected to a single-cycle sinusoidal pressure wave is computed using the present method. The constant  $\bar{b}_c$  of the FGM plate is fixed at 0.5 and the constant  $\bar{b}_\rho$  is fixed at zero, so that the wave velocity at the middle point is fixed at  $c_r = 5000$  m/s. The results are shown in Figure 4 for the stress at the middle point in the FGM plate together with that in a homogeneous plate whose wave velocity is  $c_r$ . Because the pressure wave is applied on upper surface where the wave velocity is the highest, and the wave velocity of the

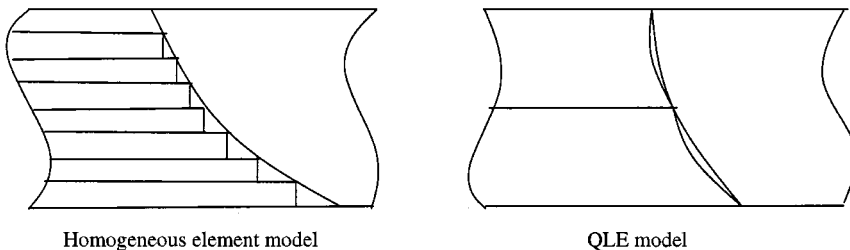


Figure 2. Two discrete models.



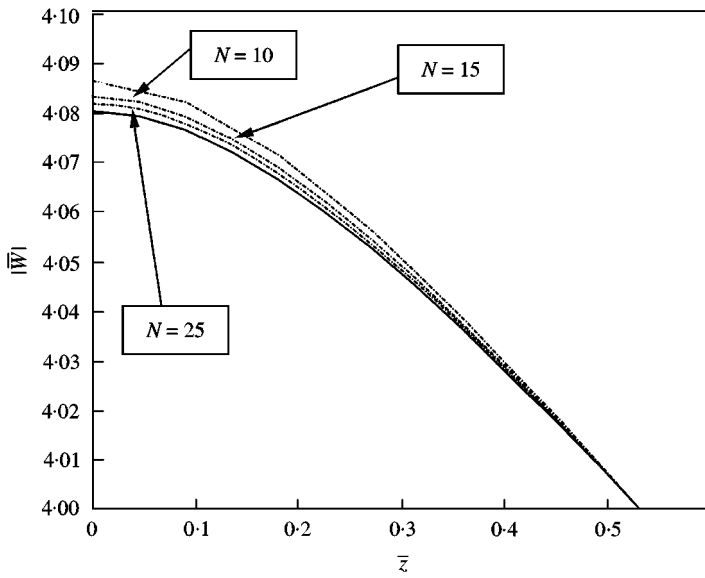


Figure 3. Comparison of results obtained by the present method (solid line) with those obtained by homogeneous method (dashed line) for a quadratic FGM plate.

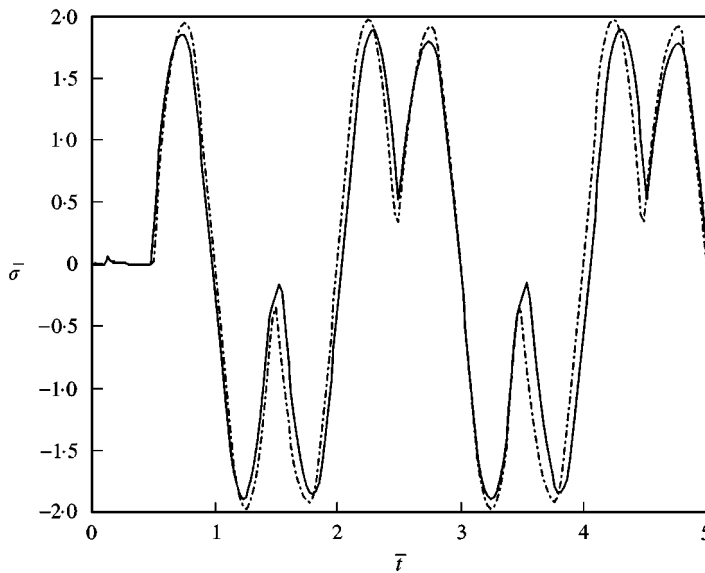


Figure 4. Comparison of time history of the stress at the middle point of a FGM (solid line) and homogeneous (dashed line) plates subjected to a single cycle of sinusoidal pressure wavelet on the upper surface. ( $\bar{\omega}_f = 6.28$ ,  $\bar{b}_p = 0$ ,  $c = c_r(1 + 0.5z/H)$ ).

FGM plate is higher than that of homogeneous plate in the upper-half portion of the plate, the stress wave propagates faster in the upper-half of the FGM plate. When the stress wave is travelling in the lower portion of the plate, the wave velocity in the homogeneous plate is higher than in the FGM plate. This is clearly evident in Figure 4 where the dashed line is lagging behind during the time  $0 < \bar{t} < 1.5$ , and then over-taking during  $1.5 < \bar{t} < 3.0$ . With

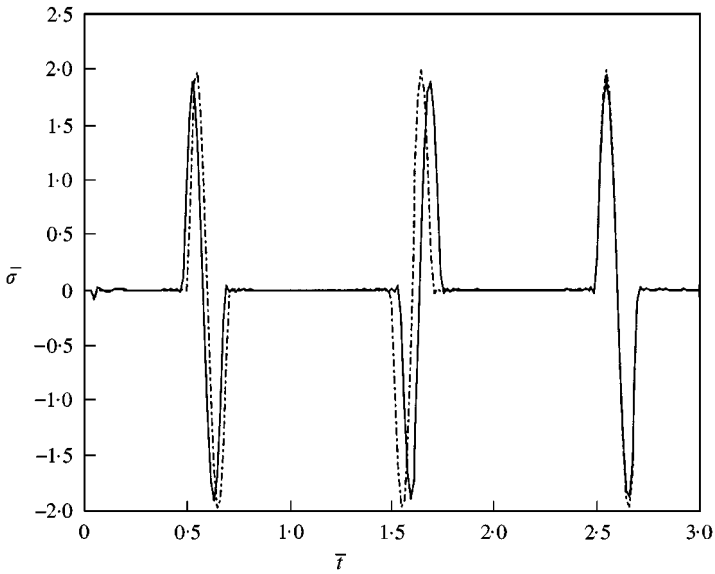


Figure 5. Same as Figure 4 but for  $\bar{\omega}_f = 31.4$ .

increasing time, the dashed line will again be over-taken by the solid line, and so on. It is also observed that the amplitude of the stress wave in the FGM plate is slightly smaller than that in the homogenous plate. This is because the pressure wave is applied on the harder surface that is capable of taking higher stress, and leaving small stress for other portion of the plate to take.

Consider a pressure wave with higher frequency ( $\bar{\omega}_f = 31.4$  and  $\bar{t}_f = 0.2$ ). Figure 5 shows the time history of the stress at the middle point of the FGM and homogeneous plate. The phenomena observed in Figure 4 can be again seen. It is more clearly shown that the stress waves change their signs whenever they hit the free surfaces of the plates.

#### 4. MATERIAL CHARACTERIZATION OF FGMS

Analytical and numerical methods are suggested for characterizing material property of FGM based on QLE method. First, the relationship between the surface displacement response and the material property of quadratic FGM plates has been analytically obtained, and the material property can be directly characterized from this closed form relationship. Then a computational inverse technique is presented for characterizing material property of an arbitrary FGM plate, using QLE method as the forward solver and genetic algorithm as the inverse operator. The efficiency of present inverse technique is demonstrated in characterizing the material property of an actual SiC-C FGM.

##### 4.1. MATERIAL PROPERTY OF QUADRATIC FGMS

Consider a quadratic FGM plate, the material property is assumed to vary in the thickness direction as defined in equation (1). The displacement in the frequency domain on upper surface can be obtained as a function of  $b_c$  and  $b_p$ :

$$W = \eta^k e^{DH}(A\phi(a, b, -D\eta) + B\varphi(a, b, -D\eta)), \quad (58)$$

where  $a, b, h$  can be obtained from equation (15),  $H$  is the thickness of the plate, and

$$\eta = Hb_c + 1. \tag{59}$$

Constants  $A$  and  $B$  can be obtained from equation (29):

$$A = \alpha B, \tag{60}$$

$$B = \frac{P_h}{c_{33}^0 \eta^{k+1} \exp(h\eta) K}, \tag{61}$$

where

$$\alpha = - \frac{(h+k)\phi(a,b,-D) + 2ah\phi(a+1,b+1,-D)}{(h+k)\phi(a,b,-D) - 2ah\phi(a+1,b+1,-D)/b}, \tag{62}$$

$$K = K_A^* \alpha + K_B^* \tag{63}$$

and

$$K_A^* = (\eta h + k)\phi(a,b,-D\eta) - \frac{2ah}{b}\eta\phi(a+1,b+1,-D\eta), \tag{64}$$

$$K_B^* = (\eta h + k)\phi(a,b,-D\eta) + 2ah\eta\phi(a+1,b+1,-D\eta) \tag{65}$$

in equation (61),  $P_h$  is the magnitude of the harmonic load

$$P = P_h e^{-i\omega t}. \tag{66}$$

The relationship between the constant  $b_c$  (for fixed  $b_\rho = 0.1$ ) and displacement  $W$  is plotted in Figure 6, and the relationship between the constant  $b_\rho$  (for fixed  $b_c = 1.0$ ) and displacement  $W$  is plotted in Figure 7. These curves shown in Figures 6 and 7 imply that for

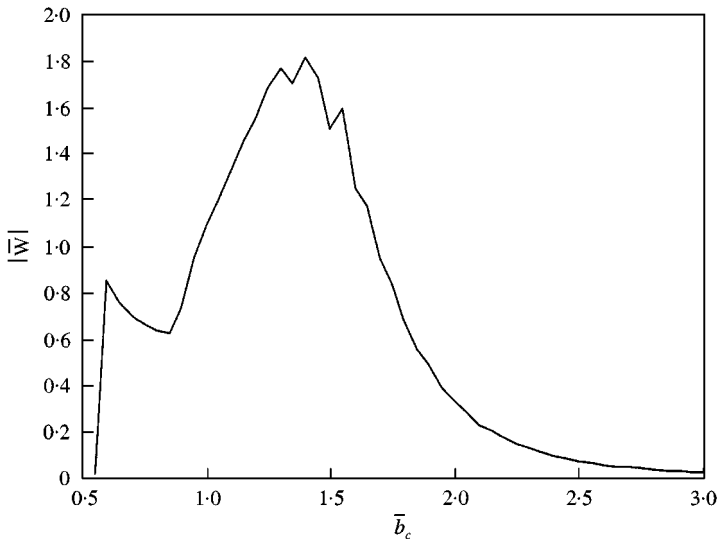


Figure 6. The relationship between displacement on the top surface and the gradient constant  $b_c$  of a quadratic FGM plate ( $\bar{\omega} = 0.5, \bar{b}_\rho = 0.1$ ).

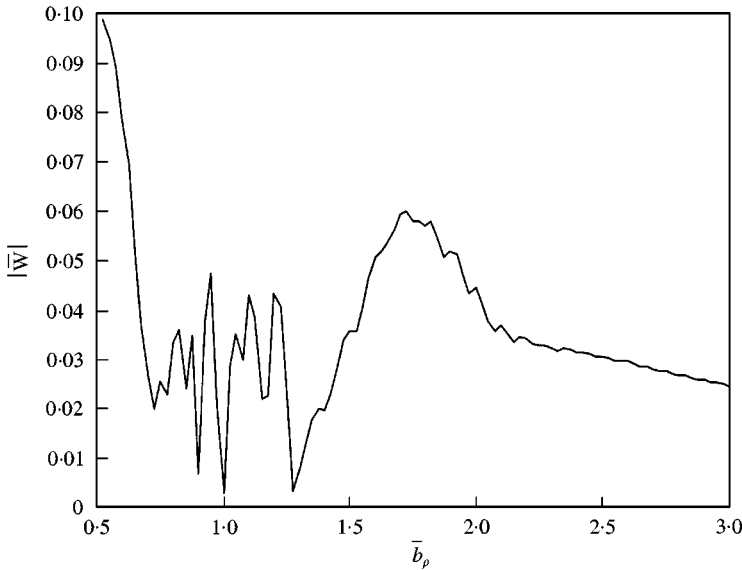


Figure 7. The relationship between displacement on the top surface and the gradient constant  $b_\rho$  of a quadratic FGM plate ( $\bar{\omega} = 2.0$ ,  $\bar{b}_c = 1.0$ ).

quadratic FGM plates, the gradient constants of elastic constant and density can be determined inversely from the measured surface displacements by a closed form, of equation (58).

#### 4.2. MATERIAL PROPERTY OF SIC-C FGM

For an arbitrary FGM plate, it can be divided into a number of QLEs. The relationship between the whole gradient constants and the upper surface displacement response data cannot be obtained in an explicit form. A computational inverse method is suggested for characterizing the material property of an arbitrary FGM plate. The QLE method is employed as the forward solver to build implicitly the relationship between displacement response on the surface and the material property, and Genetic Algorithm (GA) is employed as the inverse operator to reconstruct the gradient constants of each QLE from the upper surface displacement response data. The objective function for inverse problem can be defined by

$$\text{Minimize } \text{err}(p) = \sum_{i=1}^M \|u_i^m - u_i^c(p)\|^2, \quad (67)$$

where  $p$  represents the gradient constants, and  $u_i^m$  is the displacement response obtained from experimental measurements. In this paper, we utilize computer-generated displacement response instead of the measured one for FGM plates with given material property.  $M$  is the number of different observed points where the displacement response is sampled. In a GA run, each individual chromosome represents a candidate combination of reconstructed parameters. For each candidate combination, forward calculation has to be performed to obtain  $u_i^c$ , the displacement response subjected to the given dynamic loading. These calculated displacement readings are used to obtain the fitness value of the candidate combination. The fitness value, which is defined as equation (67), will determine the

TABLE 1

*GA search space for SiC-C FGM plate*

Parameter	Original data	Search range	Possibilities no.	Binary digit
$\bar{b}_c^1$	5.5	4.40–6.60	256	8
$\bar{b}_c^2$	4.4	3.52–5.28	256	8
$\bar{b}_p^1$	0.4	0.32–0.48	128	7
$\bar{b}_p^2$	1.0	0.80–1.20	128	7

probability of the candidate being chosen as a future parent. A FORTRAN sub-program for forward calculation using QLE is developed and interfaced with the GA main program.

Consider an actual SiC-C FGM plate as an example of the arbitrary FGM plate. The effective material property of this FGM is given by Kerner [17]. The plate is divided evenly into two QLEs. There are, therefore, four gradient constants for this whole plate, and they are denoted as  $b_c^1, b_p^1, b_c^2, b_p^2$ , respectively, where the superscripts stand for the element numbers. The original values of these four gradient constants are shown in Table 1.

The search range for the four parameters are set between  $-20$  and  $+20\%$  from the actual values as shown in Table 1. These four parameters are described and translated into a chromosome of length. In the whole search space, there are  $2^{30}$  possible combinations of these four parameters. The uniform crossover micro-GA [18] is used as the GA performance. Both the noise-free and noise-contaminated displacement responses are used for the characterization of the gradient constants. The Gauss noise of various levels is directly added to the computer-generated displacements. A vector of pseudo-random number is generated from a Gauss distribution with mean  $a$  and standard deviation  $b$ . The mean  $a$  is set to zero, and the standard deviation  $b$  is defined as

$$b = p_e \times \left[ 1/M \sum_{i=1}^M (u_i^m)^2 \right]^{0.5}, \tag{68}$$

where  $u_i^m$  is the computer-generated displacement reading at the  $i$ th sample point,  $p_e$  is the value to control the level of the noise contamination, e.g.  $p_e = 0.05$  means 5% noise. To investigate the sensitivity and stability of present inverse procedure to noise, three noise levels: 2%, 5%, and 10% are considered in this work. The characterized results are listed in Table 2. The accurate identification results demonstrate the efficiency of present inverse procedure and forward solver using QLE. Furthermore, it also should be noted that the

TABLE 2

*Characterized gradient constants for SiC-C FGM*

Parameter	Original data	Results (deviation) for different noise levels			
		Noise free	2% noise	5% noise	10% noise
$\bar{b}_c^1$	5.5	5.65(2.8%)	5.77(4.9%)	5.43(−1.3%)	5.81(5.6%)
$\bar{b}_c^2$	4.4	4.52(2.7%)	4.34(−1.4%)	4.55(3.4%)	4.76(8.2%)
$\bar{b}_p^1$	0.4	0.42(5.0%)	0.38(−5.0%)	0.38(−5.0%)	0.43(6.0%)
$\bar{b}_p^2$	1.0	0.98(−2.0%)	0.98(−2.0%)	0.94(−6.0%)	1.07(7.0%)

reconstructed results remain stable regardless of the levels of noise; even level of 10% is acceptable.

## 5. CONCLUSIONS

In this paper, a numerical method is presented for analyzing the response of FGM plate excited by a pressure wave using QLEs, whose elastic constants and mass density change quadratically in the thickness direction. A general solution of the equation of motion for the QLE is derived. This solution is used together with the boundary and continuity conditions to obtain the response of an arbitrary FGM plate both in frequency and time domain. The propagation of a stress wave in a FGM plate is computed and discussed in details.

Analytical and numerical methods are proposed for characterizing material property of FGM using the present QLE method. Firstly, the relationships between the surface displacement response and the material property of quadratic FGM plates have been obtained to characterize the material property of quadratic FGM. Then a computational inverse technique is presented for characterizing material property of an arbitrary FGM plate from the upper surface displacement response data. This technique is performed to characterize the material property of an actual SiC-C FGM. It can be found that the inverse technique could provide an accurate predication of the material property of FGM from the displacements response data measured on the surface. The present QLE method can be used as a forward solver in an inverse process for material characterization of FGM.

## REFERENCES

1. R. M. JONES 1975 *Mechanics of Composite Materials*, Scripta, Book Co., Washington, D.C., U.S.A.
2. S. W. TSAI and T. H. HAHN 1980 *Introduction to Composite Materials*. Westport, conn., Technomic Publishing Co.
3. M. SASAKI, Y. WANG, T. HIRANO and T. HIRAI 1989 *Journal of Ceramic Society of Japan* **97**, 539–543. Design of SiC/C functionally gradient material and its propagation by chemical vapor deposition.
4. R. WATANABE and A. KAWASAKI 1990 *Proceedings of the 1st International Symposium on Functionally Gradient Materials* (Yamanouchi et al., editors), 107–113. Sendi, Japan. Overall view of the P/M fabrication of functionally gradient materials.
5. G. R. LIU and J. TANI 1994 *ASME Journal of Vibration and Acoustics* **116**, 440–448. Surface waves in functionally gradient piezoelectric plates.
6. G. R. LIU, J. TANI and T. OHYOSHI 1991 *Transactions of the Japan Society of Mechanical Engineers* **57A**, 131–142. Lamb waves in a functionally gradient material plates and its transient response. Part 1: theory; Part 2: calculation results.
7. G. R. LIU and J. TANI 1992 *Transactions of the Japan Society of Mechanical Engineers* **58A**, 504–507. SH surface waves in functionally gradient piezoelectric material plates.
8. T. OHYOSHI 1993 *Mechanics Research Communication* **20**, 353–359. New stacking layer elements for analyses of reflection and transmission of elastic waves to inhomogeneous layers.
9. T. OHYOSHI G. J. SUI and K. MIURO 1996 *Proceedings of the ASME Aerospace Division* **52**, 101–106. Using of stacking model of the linearly inhomogeneous layers elements.
10. G. R. LIU, X. HAN and K. Y. LAM 1999 *Composite Part B* **30**, 383–394. Stress waves in functionally gradient materials and its use for material characterization.
11. D. S. DU 1997 *Ph.D. thesis, Harbin Institute of Technology, China*. Research on the multi-parameter inversion method of transfer operator in the stratified medium.
12. ANDREI D. POLYANIN and VALENTIN F. ZAITSEV 1995 *Handbook of Exact Solutions for Ordinary Differential Equations*. Boca Raton, FL: CRC Press.
13. N. VASUDEVAN and A. K. MAL 1985 *ASME Journal of Applied Mechanics* **52**, 356–362. Response of an elastic plate to localized transient sources.
14. E. KAUDEL and J. M. ROËSSET 1992 *ASCE Journal of Engineering Mechanics* **118**, 721–734. Frequency domain analysis of undamped systems.

15. G. R. LIU and J. D. ACHENHACH 1995 *ASME Journal of Applied Mechanics* **62**, 607–613. Strip element method to analyze wave scattering by cracks in an isotropic laminated plates.
16. G. R. LIU, K. Y. LAM and E. S. CHAN 1996 *Shock and Vibration* **3**, 419–433. Stress waves in composites laminates excited by transverse plane shock waves.
17. E. H. KERNER 1956 *Proceedings of Physical Society* **63**, 808–813. The elastic and thermo-elastic properties of composite media.
18. D. L. CARROLL 1996 *Developments in Theoretical and Applied Mechanics* Vol, XVIII, eds. H. Wilson et al., School of Engineering, The University of Alabama, pp. 411–424. Genetic algorithms and optimizing chemical oxygen-iodine lasers.